NATIONAL AERONAUTICS AND SPACE ADMINISTRATION

Technical Report 32-1536

Preliminary Investigations of Ion Thruster Cathodes

Raymond Goldstein
Eugene V. Pawlik
Liang-Chi Wen

JET PROPULSION LABORATORY
CALIFORNIA INSTITUTE OF TECHNOLOGY
PASADENA, CALIFORNIA

August 1, 1971

NATIONAL AERONAUTICS AND SPACE ADMINISTRATION

Technical Report 32-1536

Preliminary Investigations of Ion Thruster Cathodes

Raymond Goldstein
Eugene V. Pawlik
Liang-Chi Wen

JET PROPULSION LABORATORY
CALIFORNIA INSTITUTE OF TECHNOLOGY
PASADENA, CALIFORNIA

August 1, 1971

Prepared Under Contract No. NAS 7-100
National Aeronautics and Space Administration

Preface

The work described in this report was performed by the Propulsion and Engineering Mechanics Divisions of the Jet Propulsion Laboratory.

Contents

Tables

Figures

Contents (contd)

Figures (contd)

Abstract

Results of experimental and analytical studies of mercury-vapor-fed hollow cathodes for ion thrusters are presented. These studies have included the thermal and electrical characteristics of the cathodes. It is shown that the primary electron emission mechanism is thermionic when sufficient low work function material is present in the cathode. The cathode temperature is determined by the current demanded by the external circuit and the work function of the emitting surface. The result is an increase in cathode temperature as the low work function material is depleted. In addition, attempts to reduce cathode temperature by changes in external thermal coupling result only in increasing the power extracted from the discharge. These phenomena affect overall thruster performance.

Preliminary Investigations of Ion Thruster Cathodes

I. Introduction

The advent of mercury-vapor-fed hollow cathodes (Ref. 1) for ion thrusters appeared to reduce some of the durability problems of oxide cathodes (Ref. 2), permitting thruster endurance testing on an orbiting satellite (Ref. 3). It was found that excessive cathode operating temperature, which apparently adversely affected cathode integrity, could be reduced to satisfactory levels by proper selection of orifice and overall cathode size (Refs. 4–6). It was felt, generally, that cathode endurance was no longer a problem for ion thruster operation.

Unsatisfactory variations in cathode operation have occurred, however, during the solar electric propulsion system tests (Ref. 7) presently being conducted at JPL. These have led to a careful reexamination of thruster hollow cathode operation, with emphasis on the identification of the electron emission process. This report presents the initial results of that study, which is still currently being carried out.

Several workers have investigated various aspects of flowing-gas, hollow cathode discharges. Lidsky et al. (Ref. 8) studied the energy balance of their discharges and concluded that the ion current to the cathode was a small fraction of the total cathode current. Hence it was felt that electron emission was primarily thermionic, possibly with some field enhancement.

Delcroix et al. (Ref. 9) measured the detailed temperature distribution along the cathode and tried correlating these measurements with the gas pressure drop along the inside of the cathode. Their conclusion was that the location of the arc attachment region within the cathode is determined by the gas flow rate and certain properties characteristic of the gas.

Our results are in agreement with both of these investigations and provide a specific detailed description of the ion thruster mercury-vapor-fed hollow cathode.

II. Apparatus

Tests were conducted on several cathodes operated both in a diode test setup and in an ion thruster. Diode experiments were conducted with the cathode emitting to a flat anode surface within a bell jar vacuum facility. Ion thruster tests were conducted in a vacuum tank 0.914 m in diameter and 2.13 m long. Operating pressures were less than 1.3×10^{-3} N/m^2 (10^{-5} torr) for both facilities.

A. Cathodes

The mercury-fed hollow cathode examined in this study utilizes a hollow tube which is supplied with gaseous mercury from a porous tungsten vaporizer. A flow-restricting orifice may be located at the cathode face.

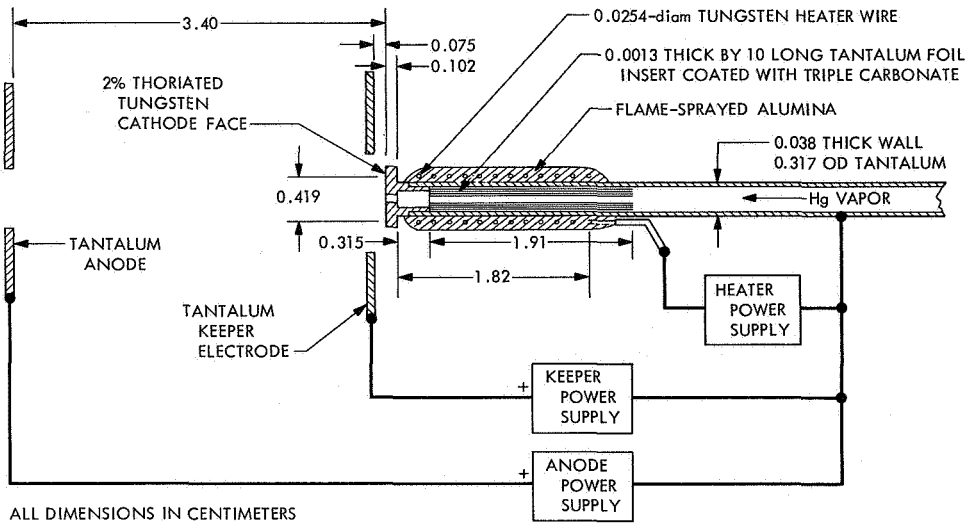

Fig. 1. Standard cathode and bell jar power supplies

Cathode interior pressure is normally on the order of 1.33×10^2 N/m^2 (1.0 torr) during operation. The cathode discharge can be initiated in several different ways. Two ways that were used in this investigation are:

(1) Heating the cathode until a low work function material emits electrons thermionically. Then, with a sufficient Hg flow a low voltage arc is struck to a nearby keeper electrode.

(2) Striking a high-voltage arc between the cathode and keeper electrode or anode.

Two types of cathodes were used in this work: the standard cathode, which is the type normally used in the ion thruster, and a tube cathode. These cathodes and their bell jar test setup are described in detail below.

1. Standard cathode. This type of cathode in a bell jar test setup is shown in Fig. 1. The cathode consisted of a thoriated tungsten face containing an orifice. The face portion was electron-beam-welded to a tantalum tube which was wrapped with a heating element. Flame-sprayed Al_2O_3 was used as the electrical insulator for this heater. An insert consisting of tightly rolled tantalum foil coated with triple-carbonate (barium, strontium, calcium) was placed within the tube. A nominal 20 micrograms of the carbonate mixture was normally used in this insert; additional face and interior coatings were used during some tests. Several variations existed in the cathode geometry. Orifice diameters of 1.02, 1.14, and 1.27 mm were used, and there were variations in the heater element heat shielding. In addition, some cathodes contained a grooved surface on the tantalum tube to permit uniform heater wire spacing.

Cathode temperatures were measured with 5/26% rhenium-tungsten thermocouples and an optical pyrometer. A thermocouple was located on the cathode face during operation in both the diode and thruster experiments. The bell jar test setup permitted viewing of the cathode with the pyrometer.

2. Tube cathode. This cathode in a bell jar test setup is shown in Fig. 2. The 1.2-mm-ID tungsten tube with a 0.08-mm wall was cemented into a larger tantalum tube. The thin wall made possible pyrometer measurements of the temperature distribution along the cathode. Tests

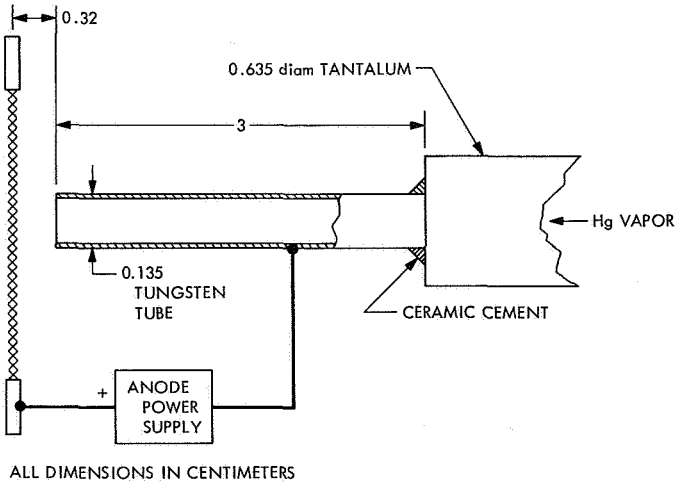

Fig. 2. Tube cathode and bell jar power supply

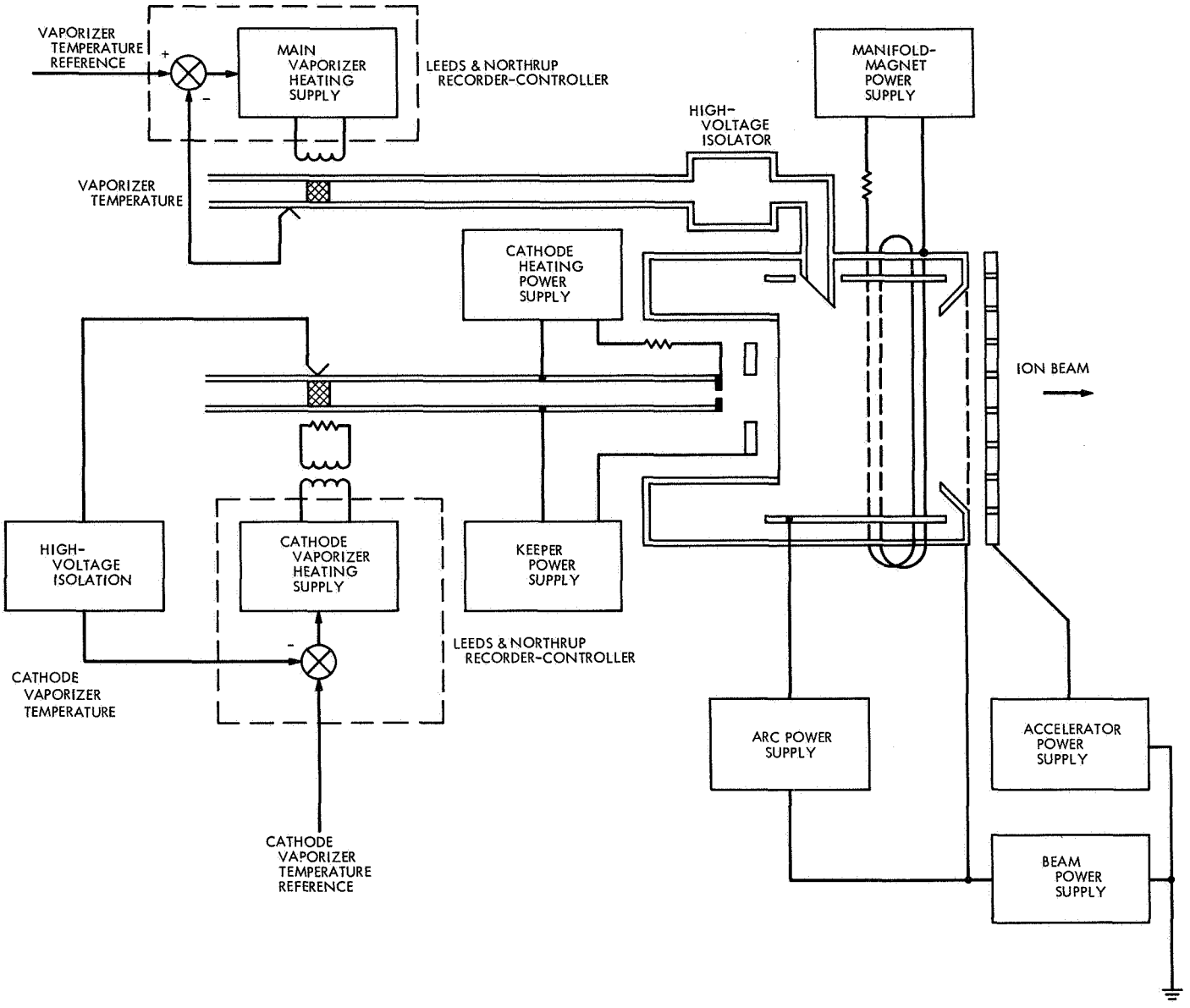

Fig. 3. Ion thruster schematic

were conducted with and without a triple carbonate coating present on the cathode interior.

B. Thruster

The basic elements of electron bombardment ion thruster, power supplies, and control loops are shown in Fig. 3. The nominal operating level for the 20-cm-diam ion thruster used in the program is 1000–2000 W (0.5–1.0 A beam current at 2000 V net acceleration) of throttlable output beam power at a constant specific impulse near 4000 s. The details of thruster construction and performance can be found in Refs. 10 and 11. A combination keeper-baffle was used (flat baffle, 4.70 or 4.32 cm diam). The cathode used contained a 1.14-mm-diam orifice, grooved body, and two wraps of heat shielding.

III. Results and Discussion

Four tests were conducted to determine the role of triple carbonate in the emission process. These include operation of (1) a tube cathode as a diode, (2) a standard cathode as a diode, (3) a standard cathode in a thruster, and (4) a standard cathode as a diode with additional instrumentation for thermal analysis.

A. Tube Cathode

Characteristics of the tube cathode have been studied primarily with no triple carbonate present. Some preliminary results of the effects of such coatings are available, and a more detailed investigation is currently in progress.

The tube cathode (both uncoated and coated) is heated by the discharge over a distance many diameters long, the hottest portion occurring a few diameters from the tip. The temperature distribution depends on the arc current and mercury flow rate and is similar to that observed by Delcroix et al. (Ref. 9). In a typical case, an uncoated cathode operates at about 1600°K at its hottest portion with 45 mA arc current. The arc voltage is 300 V, and the Hg flow rate is about 0.5 g/h. Arc current greater than 100 mA quickly destroys the cathode because of the high temperatures produced, so these tests are restricted to relatively low currents.

The arc currents observed are up to three orders of magnitude greater than the pure thermionic emission available from the bare tungsten. Simple thermionic emission is clearly not involved here, and other mechanisms must be considered. The various possibilities for emission are discussed only briefly here. For a more detailed discussion see Ref. 12.

Field emission or field-enhanced thermionic emission requires electric fields of 10^6–10^7 V/cm at the cathode. Such fields are possible if the cathode sheath is sufficiently thin. Photoemission requires a sufficient flux of photons of energy greater than 4.5 V (wavelengths less than 275 nm). Likewise, the secondary emission processes resulting from atom or ion impact require a sufficient flux of particles in an appropriate state.

The calculation of the contribution of each of these processes requires detailed knowledge of the plasma properties within the cathode, surface properties of the cathode, and the yield of electrons per primary particle for each process. Rather than attempt such a difficult task here it will be sufficient to point out merely that the cathode currents observed must represent the total contribution of these processes. That is, these secondary emission processes can provide current levels of the order of tens of milliamperes for the tube cathode being considered or *current densities of no more than a few tenths ampere per cm²*, at an arc voltage of 300 V for temperatures of the order of 1500–2000°K.

The preliminary results of tests on triple-carbonate-coated tube cathodes show considerably different properties. The current levels are of the same order as thermionic emission currents from oxide cathodes. For example, a coated cathode operates at about 1800°K with 50 A/cm² current density at 18 V.

B. Standard Cathode

We have found that the standard hollow cathode exhibits two extreme sets of thermal characteristics, which we have called the cold and hot modes, as shown in Fig. 4. The temperatures shown were measured with an optical pyrometer looking at the cathode head-on. The magnification of the pyrometer telescope was sufficient to allow measurement of temperatures in the cathode interior. The curves show measured temperature as a function of arc plus keeper current (the latter normally is 1 A) and represent typical results for a 1.04-mm-diam orifice cathode. Emissivity corrections (Ref. 13) have been applied to the observed face temperatures. Radiation from the interior should be very close to black body emission, and hence such corrections were not applied to internal temperatures. It should be pointed out,

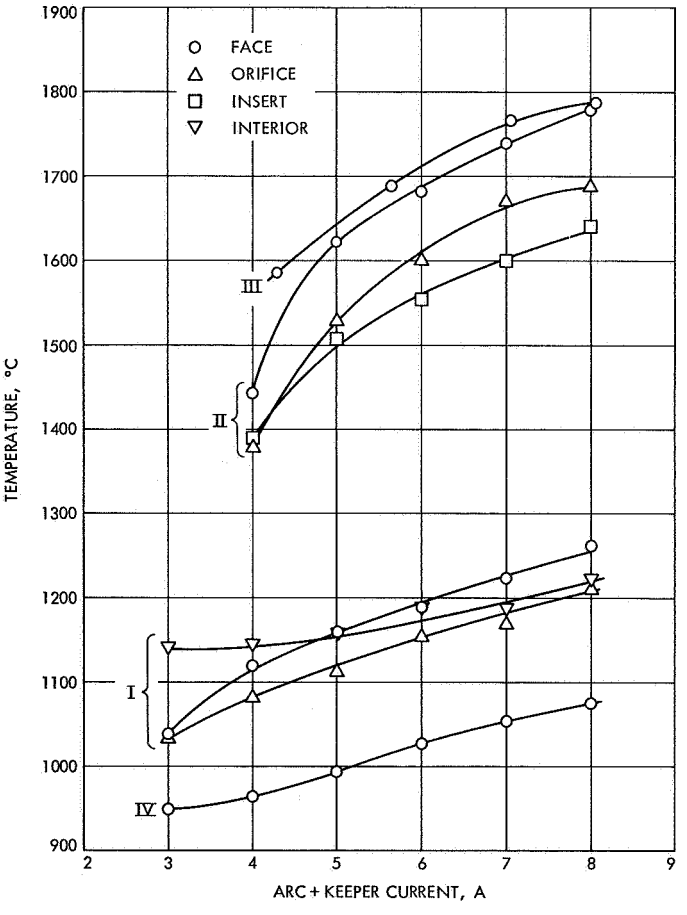

Fig. 4. Cathode operating temperatures in bell jar

however, that internal reflections and aperture effects may result in measured internal temperatures differing from their true values. The data of Fig. 4 are presented to indicate the overall nature of the temperature variations. The quantitative calculations presented in Section III-D involve the thermocouple measurements, which we feel are more reliable although more difficult to obtain.

A freshly prepared cathode operates in the cold mode shown by curves I in Fig. 4. The face, orifice, and interior temperatures are separately given. Note that the orifice is coolest and that the face is cooler than or about the same temperature as the interior. The current densities in this case are of the same order as would be expected for thermionic emission from an oxide cathode.

A photograph of the cathode operating in this mode (at 6 A total current) is shown in Fig. 5a. The bright crescent is the lateral surface of the orifice, viewed at an angle of 20 deg. It appears brighter than the face because of the difference in effective emissivities of the two surfaces discussed above. Note that details of the interior structure are not distinct in this mode.

After a period of operation (see below), the mode of operation of some cathodes slowly changes to give temperatures shown by II in Fig. 4. Note that the temperatures are shifted upward, with the face now clearly the hottest. The temperatures in this hot mode are excessive for maintenance of long life of the cathode and cathode heater. In addition, for given current and mercury flow rate, arc and keeper voltages are slightly higher in this mode compared to the cold mode. Hence the efficiency of operation is lower in the hot mode. Also, it is possible in this mode to see the interior structure clearly. Figure 5b is a photograph of the cathode operating in the hot mode (at 6 A total current). The outer crescent is again the surface of the orifice, and the inner crescent is the now incandescent end of the insert.

We have experienced great variations in the transition time from cold to hot mode. Some cathodes have exhibited significant change within several hours of operation. Others have operated for over 50 h with only slight change in characteristics. The reasons for this variation in transition are as yet unclear but are likely to involve the lack of uniformity that must result from preparation of the cathodes.

We have been unable to return a hot-mode cathode to low-temperature operation either spontaneously or by restarts. However, application of triple carbonate to the cathode interior (by hypodermic syringe through the orifice) does result in cool-mode operation. The resulting measured face temperature is shown by IV in Fig. 4 and represents an extreme of cool-mode operation. The insert

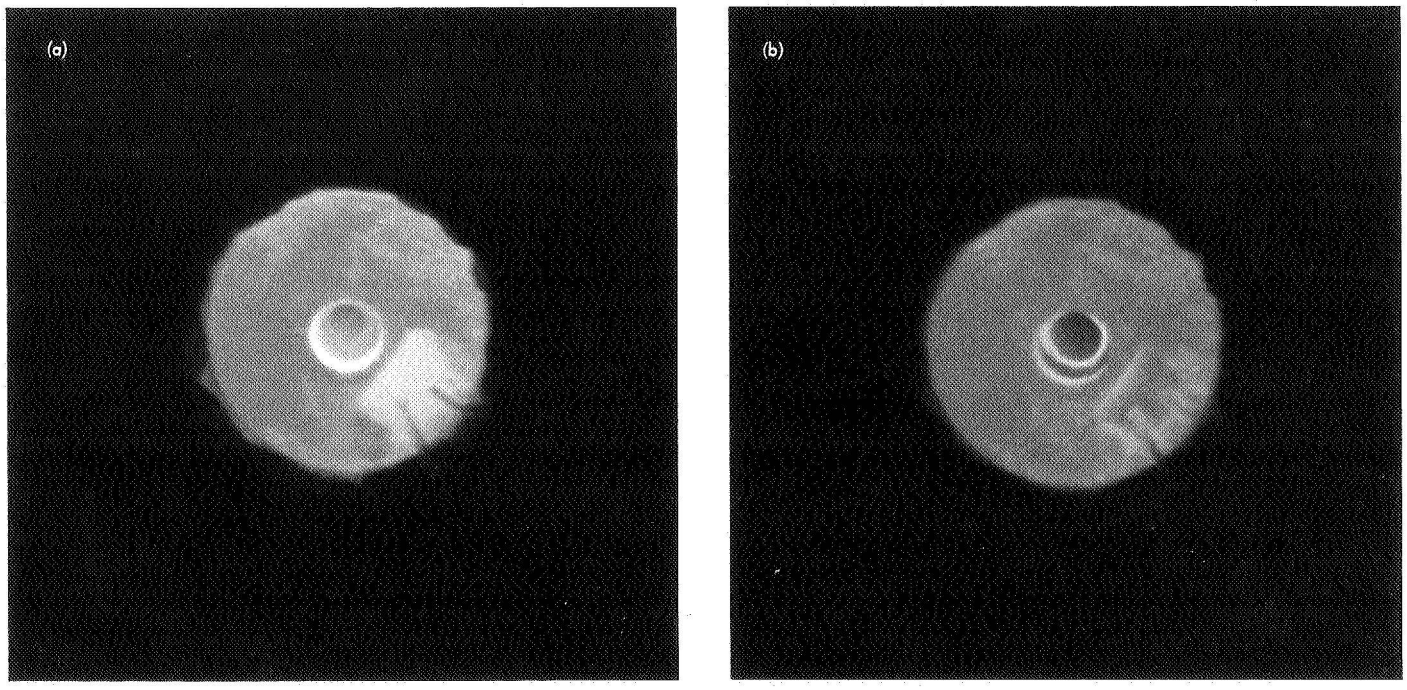

Fig. 5. Photographs of operating cathode

of the cathode was then replaced by a new insert with no carbonate coating (the interior of the cathode itself was thoroughly cleaned as well). The face temperature measured for this case is shown by III in Fig. 4. This is obviously the extreme of hot-mode operation.

C. Thruster Tests

A cathode with a 1.14-mm-diam orifice was operated in a 20-cm-diam ion thruster during several tests. Thruster operation with two electron baffle diameters, 4.32 and 4.70 cm, was examined. Measured cathode face temperatures are presented in Fig. 6 for several runs. The cathode was initially used with a 4.70-cm-diam baffle for 66 h of continuous operation. The cathode was exposed to atmosphere for about two months and then was reinstalled with less heat shielding in an attempt to reduce the operating temperature. A higher operating temperature was observed to result, however. The cathode face was next coated with a triple-carbonate solution and run in the thruster. The baffle diameter was then decreased in order to reduce the propellant flow through the cathode. Neither of these changes was found to influence measurably the operating temperature of the cathode. As in the case of the bell jar operation, injecting a solution of triple carbonate into the cathode interior did reduce the face temperature significantly. The discharge chamber losses were also appreciably reduced by the addition of this low work function material, as indicated in Fig. 7. The lower discharge losses are believed to be a result of (1) less energy extracted from the arc discharge, (2) a redistribution of the mercury propellant, and (3) less arc voltage applied to the arc. The reduced flow through the cathode was necessary in order to maintain the arc voltage at 35 V. This resulted in more of the propellant being introduced directly into the arc chamber by the main vaporizer in order to maintain a constant propellant total flow rate. A higher percentage of the propellant flow directly introduced into the arc chamber usually results in lower arc chamber losses (Ref. 14).

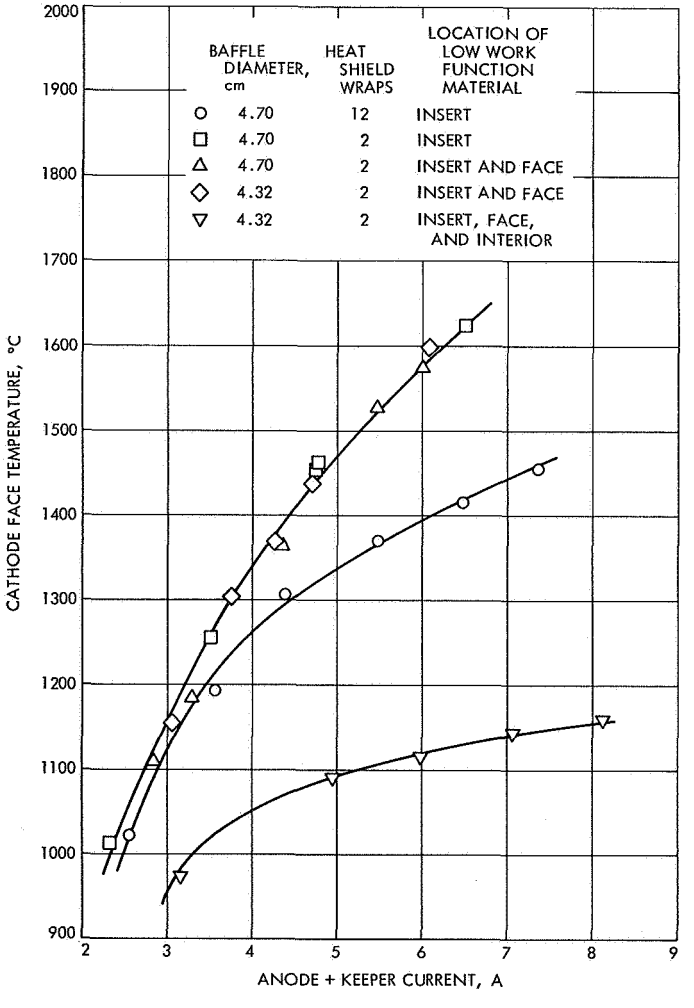

Fig. 6. Effect of barium oxide on cathode operating temperature

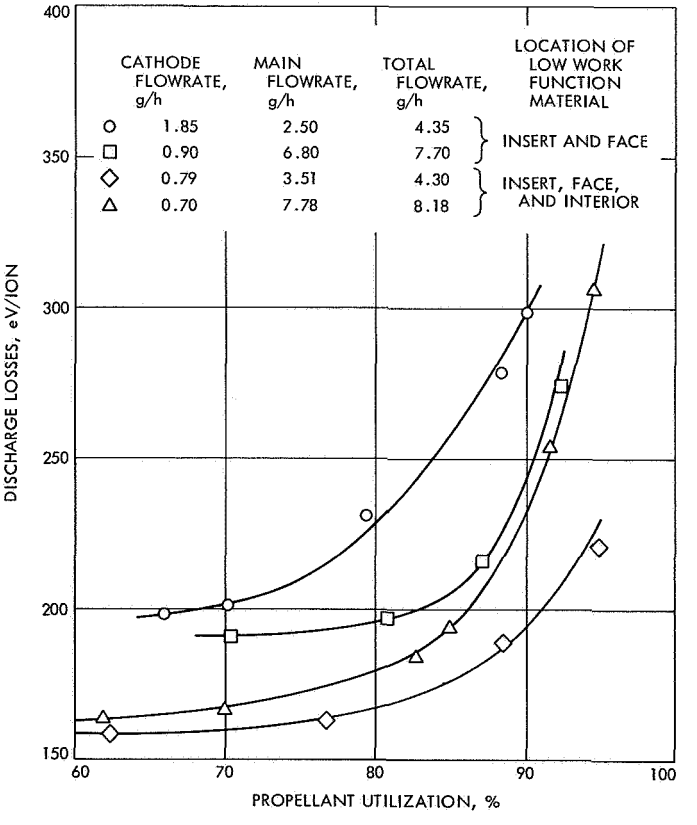

Fig. 7. Effect of barium oxide on thruster discharge chamber losses

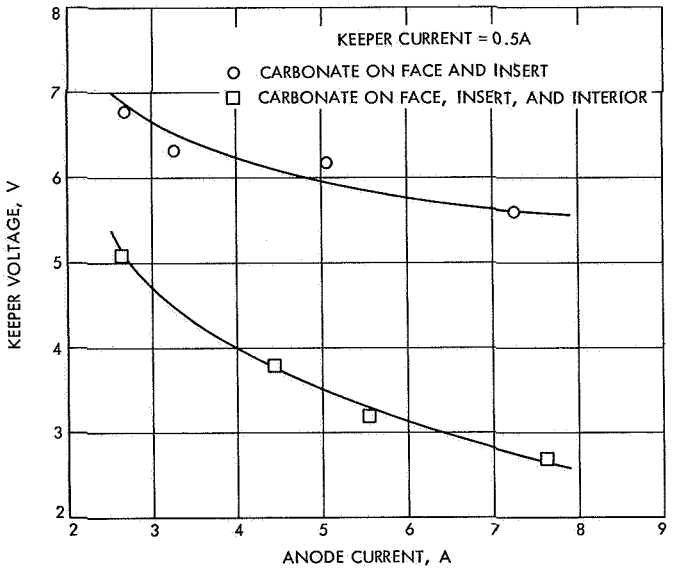

Fig. 8. Effect of barium oxide on keeper electrode voltage

The keeper voltage is shown in Fig. 8 as a function of the anode current for both the coated and uncoated cathodes. Since this voltage might be expected to be representative of the plasma potential near the region of the cathode, greater ion bombardment heating of the cathode would be expected as this voltage increases. Also, since a greater portion of the total arc voltage and power is developed near the cathode, a decrease of voltage and power occurs in the remainder of the thruster.

D. Thermal Analysis

Detailed temperature distributions were measured with 5/26% rhenium-tungsten thermocouples located on standard 1.04- and 1.27-mm-diam-orifice hollow cathodes operating in the bell-jar facility. To simplify the analysis, no heat shielding was used for most of these thermal studies.

Temperatures were measured with the cathodes heated externally by their electrical heaters as well as being self-heated by the discharge. The former was used as a calibration between the analytic model and the measurements, representing a case for which the total heat input to the cathode was known. Then the model was used to match the measured temperature distributions for the self-heating cases.

The thermal balance of the system was studied using a 34-node mathematical model; 29 nodes represented various parts of the cathode and 5 nodes represented the surrounding environment. The basic nodal energy balance relationship for each node of the system is of the form

$$P_i - \sum_{j=1}^{N} K_{ij} (T_i - T_j) = A_i \epsilon_i (\sigma T_i^4 - G_i) \qquad (1)$$

where

P_i = net thermal energy input to node i through electrical heating or cathode self-heating

K_{ij} = thermal conductance between nodes i and j

A_i = radiating surface area

ϵ_i = total hemispherical emittance of surface i

G_i = total infrared irradiation flux to node i

σ = Stefan–Boltzmann's constant

T_i = *nodal equilibrium temperature*

The mathematical model was evaluated numerically using the thermal analyzer program HEAT. The temperature distribution of the cathode can be calculated when the heating power and a boundary nodal temperature are given.

This analytic model was used to determine the total cathode self-heating power, and to study the effects on temperature distribution of the specific location of this heating and the location of the electron emission. This analysis has allowed us to determine in some detail the locations of these processes.

Figure 9 shows typical cathode temperature distributions for a fixed face temperature measured for a 1.27-mm-orifice cathode operating with external heater and with self-heating only. For the latter, the total power input is calculated from the model to be 19 W. To achieve the same face temperature, external power of 39 W is required. Hence it is incorrect to assume, as is usually done (Ref. 6), that for a given face temperature self-heating power is equal to the electrical heater power to produce that temperature. Note also from Fig. 9 that the highest temperature occurs at different locations for each distribution. This electrical heater design therefore does not heat the cathode in the most efficient manner. Figure 10 summarizes the comparison of heating power required for a given face temperature for the two methods of heating. Over the entire range of discharge current the self-heating power is significantly less than the external electrical power.

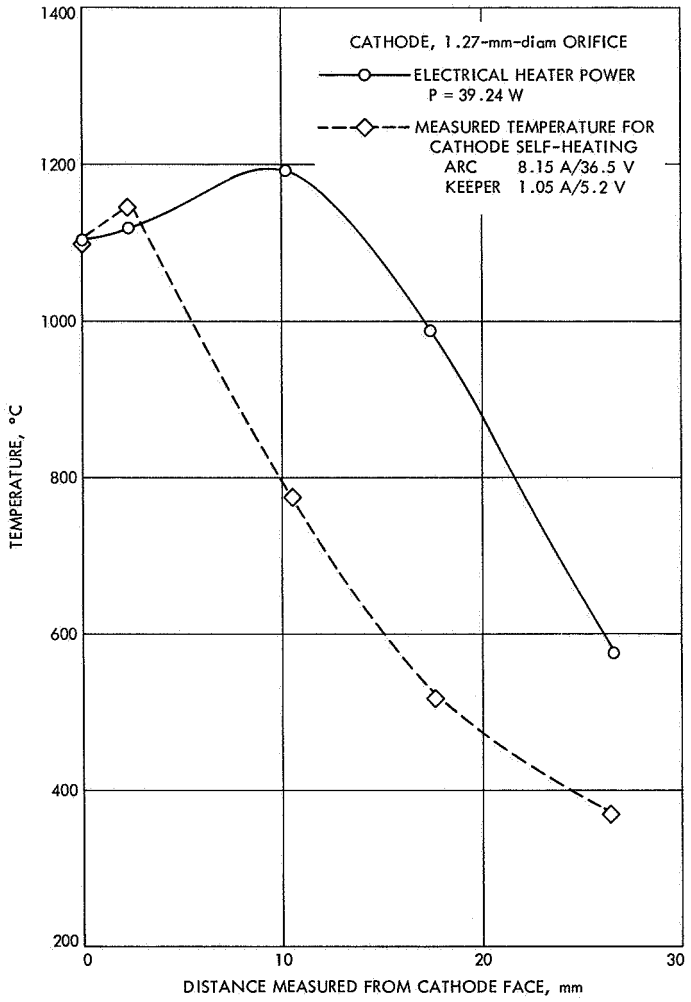

Fig. 9. Temperature distributions for external heating and self-heating of 1.27-mm-orifice cathode

The effective self-heating cathode power has been considered to be expressed by the following equation:

$$P = Q - J\phi \qquad (2)$$

where

P = effective self-heating cathode power, W

Q = total cathode heating

J = total discharge current, A

ϕ = cathode work function:
1.5 V for barium carbonate
2.6 V for thoriated tungsten

The specific locations of heating Q and cooling $J\phi$ due to electron emission affect the temperature profile near the cathode tip, so by comparison of measured and calculated temperature profiles these sites can be determined. Applying the established mathematical thermal model of the cathode and the measured boundary condition, temperature profiles were calculated for a bare standard cathode (orifice size, 1.27 mm) with various distributions of 19 W total effective self-heating power.

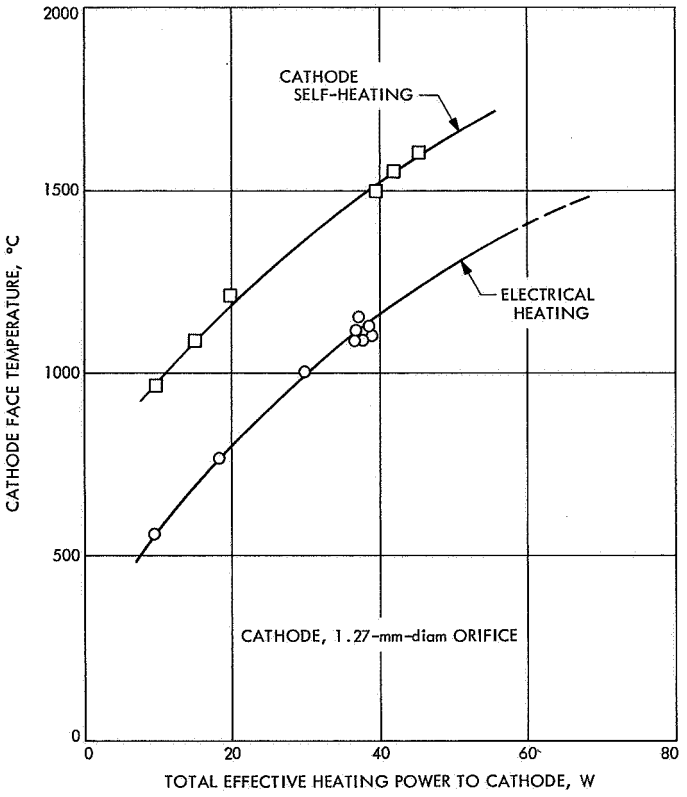

Fig. 10. Comparison of external and self-heat power for 1.27-mm-orifice cathode

Figure 11 illustrates the temperature profiles of the cathode tip region for five power distribution combinations:

(1) Power input and electron emission both occurred at the cathode face.

(2) Power input and electron emission both occurred at the orifice.

(3) Power input and electron emission were uniformly distributed over the face, the orifice, and the interior wall.

(4) Power input was concentrated at the interior surface while electron emission occurred at the cathode face.

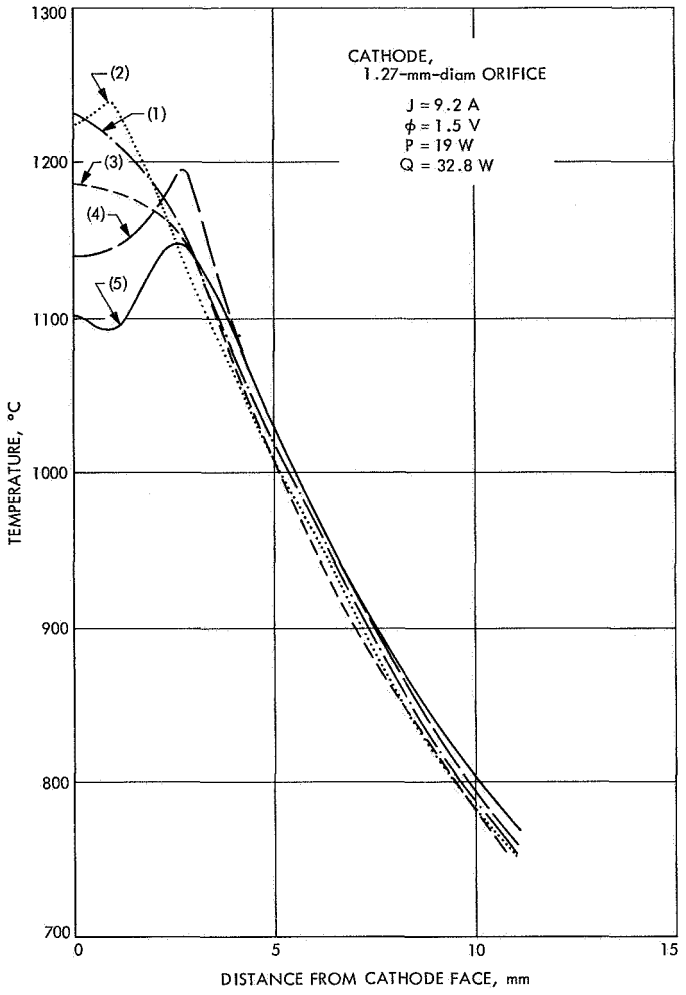

Fig. 11. Effects of heating and cooling locations on cathode temperature distribution

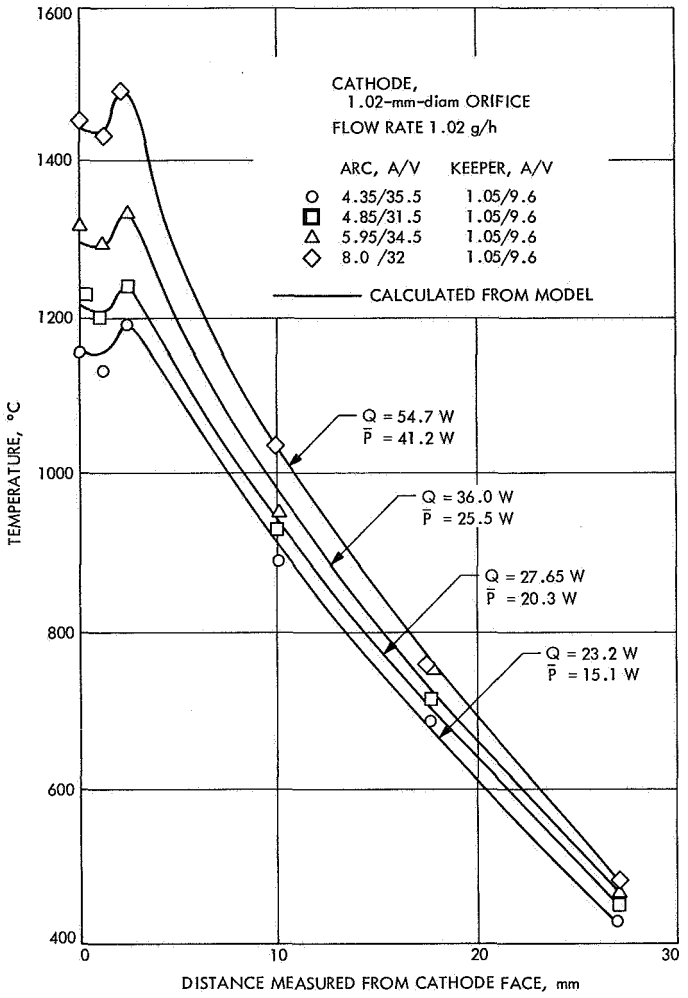

Fig. 12. Calculated and measured cathode temperature distributions

(5) Power input was distributed between the interior and the insert according to the exposed area ratio (9 to 1), and electron emission occurred at the orifice.

As can be seen from Fig. 11, the distribution of power input and emission sites affects very strongly the temperature distribution in the tip region (approximately 3 mm from the cathode face, including the face, the orifice, the interior, and the insert). Along the tantalum cathode tube, the temperature profile appears to be a function of the effective self-heating power level P only and is not greatly affected by the distribution. If the temperature gradients at the cathode tip region are accurately measured, a detailed thermal analysis can be applied to determine the emission sites and the power input distribution.

Our temperature measurements on cool-mode cathodes agree most closely with curve (5), representing emission from the orifice and heat input in the interior. The data are definitely inconsistent with curves (1) and (3), ruling out those possibilities. Because of the very low plasma density at the face (see Section III-E), we rule out emission from the face and hence case (4). We therefore conclude that electron emission occurs at the orifice and heating occurs in the interior. However, with respect to the latter we do not completely rule out the possibility of heating occurring in part or entirely at the orifice.

Figure 12 compares the temperature measurements of a 1.04-mm-diam-orifice cathode operated at 1.02 g/h flow rate to the analytical distribution, assuming electron emission concentrated at the orifice with 10% power input applied to the insert and 90% to the interior cavity

surface, as in case (5) above. The net effective heating power P and total power Q calculated from the model by determining a best fit to the data are also presented.

The values of Q thus determined can be used to estimate an upper bound for the ion current to the cathode in each case. The power P_i delivered to the cathode by ion current J_i is given by

$$P_i = (V_i + V - \phi) J_i \tag{3}$$

where V_i is the ionization energy of the neutral atom, and V is the ion kinetic energy. If all of the power delivered to the cathode is due to ion bombardment, then

$$J_i = \frac{Q}{V_i + V} \tag{4}$$

Table 1 presents values of ion current calculated from Eq. (4) using the Q's given in Fig. 12. The keeper voltage was used for the ion kinetic energy V in these calculations. Table 1 shows that the calculated ion currents are no more than 20–30% of the total discharge current. This result is in agreement with the observations of Lidsky et al. (Ref. 8), mentioned previously. Therefore, contributions to the total emission by ion bombardment can be no more than 20–30% of the total discharge current.

Table 1. Estimated ion current to cathode

Total current J, A	Total power Q, W	Ion current J_i, A
5.4	23.2	1.16
5.9	27.65	1.38
7.0	36.0	1.8
9.05	54.7	2.73

Note that if any other heating mechanisms, such as radiation from the plasma, are important, the numerator of Eq. (4) would be correspondingly reduced, thereby reducing J_i from the values given in Table 1. Exact calculation of the radiative contribution is difficult since detailed knowledge of the plasma properties must be known. However, reasonable rough estimates indicate this contribution could be at least 10% of the total power.

We have studied in some detail the overall thermal characteristics of the cathode. Changing the thermal characteristics of the cathode by applying heat shield wrappings on the external surface greatly reduces the heater power required to attain starting temperature. For example, a nude cathode requires approximately 39.2 W electrical heating for the cathode face temperature to reach 1100°C. If heat shield wrappings are applied, the same cathode face temperature needs only about 20 W electrical heating. This indicates that the heat shield reduces the effective cathode emittance to half its value. During arc operation, the self-heating cathode power also appears to be dependent on the overall cathode thermal characteristics. In other words, once the orifice size, the operational mode, the flow rate, and the total discharge current are fixed, the cathode temperature tends to attain a certain value irrespective of the thermal characteristics of the cathode, and changes in heat shielding, radiating area, and conduction path affect only the heating power extracted from the discharge.

Although the available data are not sufficiently accurate for quantitative analysis, we have observed that, all else remaining the same, the presence or absence of heat shield affects face and interior temperatures very little while changing significantly the power extracted from the discharge. In addition, we have measured cathode temperatures with an arc running both without external heat, as in normal operation, and with external heat applied. These measurements were analyzed by the analytic model to determine the power extracted from the discharge in each case. The results are shown in Table 2. Note that with external heating applied, the keeper voltage decreases slightly and about 13% less power is extracted from the discharge. In other words, the cathode extracts the power from the discharge to attain a temperature sufficient to emit the required current.

Table 2. Power extracted by cathode from plasma

Arc, A/V	Keeper, A/V	External power, W	Face temperature, °C	Power extracted Q, W
8/13	1.05/11.1	0	1670	59.2
8/13	1.05/10.5	36.4	1750	51.5

E. Electron Emission

Our analysis of the results of these studies leads us to the following explanation of the operation of the hollow cathode. The electron emission process is primarily thermionic, occurring from low work function surfaces. The cathode is heated by ion bombardment to a temperature sufficient to emit the current demanded by the external circuit. The balance between this heating, radiative and electron cooling, and conduction along the

cathode determines the details of the cathode temperature distribution.

The analysis shows that most of the ion bombardment heat input is in the cathode interior, other parts being heated primarily by conduction. Since the electron emission cooling is appreciable, we expect the emitting region to be coolest. Hence, if the emitting region moves from one part of the cathode to another, a change in temperature distribution results. For example, if the orifice is the emitting surface we would expect the orifice to be cooler than the interior. On the other hand, emission from an interior surface results in that being cooler than the face and orifice.

During startup of a fresh cathode, some low work function material is diffused from the insert to the orifice region. Arc operation will then involve electron emission from the orifice and hence cool-mode operation. If the insert can continue to supply material to the orifice as rapidly as it is depleted, the cathode should remain in this mode.

If, however, sufficient oxide cannot be provided, the cathode temperature will rise to maintain the arc current constant. (We have generally operated the cathodes with current-limited power supplies.) The arc voltage may also increase slightly at this time. Eventually there is insufficient coating at the orifice, and the arc attachment region moves into the interior of the cathode until it reaches the end of the insert. This partially depleted oxide reservoir requires an increase in temperature to maintain the current. The cathode is now in the hot mode, with all temperatures higher than previously and the face and orifice hotter than the interior. In this mode arc and keeper voltages are slightly higher because of the increased ion bombardment heating required as well as the increased length of arc within the cathode interior (Ref. 9).

Application of triple-carbonate mixture to a cathode which operates in the hot mode restores low work function material to the orifice region. The cathode will then operate in the cool mode as long as a sufficient amount of the material remains there.

Note that in order to draw the available current, space charge neutralization by the plasma within the cathode is necessary. The plasma density at the face is too low for this, and hence emission does not occur there. One role of the cavity of the hollow cathode is thus to provide a region of high plasma density for that purpose. An additional role of the cavity appears to be to contain partly the alkaline oxide vapor given off by the insert.

Some pertinent aspects of the alkaline oxide low work function material should be briefly discussed here. The triple-carbonate (barium, strontium, calcium) mixture initially deposited in the insert is eventually decomposed thermally during cathode operation to a triple-oxide complex. The work function of this material is very sensitive to the presence of impurities and its physical state, but 1.5 V is typical of reported values. The hollow cathode, however, presents a situation in which a metallic surface is in contact with the alkaline oxide vapor. Hence the effective work function of the emitting surface is dependent on the work function of both the bare surface and the oxide as well as their temperatures and the oxide vapor pressure. The apparent work function of the emitting surface can therefore take on values anywhere between 1.5 and 2.6 V (for thoriated tungsten). (For a detailed discussion of this problem see, for example, the work of Levine and Gyftopoulos, Ref. 15.)

Note from Fig. 4 that temperatures for initial cool-mode operation lie between the two extremes involving no oxide coverage (III) and heavy oxide coverage (IV). This would indicate that "normal" cool-mode operation involves only a partial oxide coverage.

IV. Conclusions

We have shown that detailed temperature measurements in conjunction with an analytic model of the hollow cathode allow a detailed description of cathode operation. From the results of tests performed on various cathodes we conclude:

(1) The primary electron emission mechanism is thermionic when sufficient low work function material is present.

(2) The cathode is heated (mostly by ion bombardment) to a temperature sufficient to emit the current demanded by the external circuit.

(3) The detailed temperature distribution of the cathode is determined by a balance of the plasma heating in the interior, radiation from the exterior, electron-cooling from the emitting region, and conduction along the cathode.

(4) For a given total arc current, attempts to reduce cathode temperature by changes in the external

thermal coupling, either by increasing the cathode size or reducing its heat shielding, will affect only the amount of power extracted from the plasma and should therefore be ineffective. That is, increasing the heat flow from the cathode will be automatically compensated by an increase in the power extracted from the plasma.

(5) The relatively high-density plasma within the cathode is necessary for space charge neutralization to allow high currents to be drawn.

(6) Depletion of low work function material in the cathode results in higher operating temperatures.

(7) Considerably less self-heating power is required to produce a given cathode face temperature than is required by the external heater to produce that same temperature.

(8) When operated in a thruster these phenomena affect overall thruster performance. Specifically, depletion of alkaline oxide material in the cathode decreases discharge chamber operating efficiency and increases cathode temperature and cathode mercury flow rate.

These conclusions, which have been derived from studies on a specific cathode design, will be verified by further experiments on other cathode designs. If supported by these planned experiments, the conclusions reached here may be used as criteria for improvement of thruster hollow cathode design.

References

1. Kemp, R. F., and Hall, D. F., *Ion Beam Diagnostics and Neutralization,* Final Report, NASA Contract NAS3-7937, TRW Systems, Redondo Beach, Calif., Sept. 1967.

2. Kerslake, W. R., *Oxide-Cathode Durability in Mercury Electron-Bombardment Ion Thrustor,* NASA TN D-3818, National Aeronautics and Space Administration, Washington, Feb. 1967.

3. Goldman, R. G., Gurski, G. S., and Hawersaat, W. H., *Description of the SERT II Spacecraft and Mission,* NASA TM X-52862, National Aeronautics and Space Administration, Washington, Sept. 1970.

4. Pawlik, E. V., and Fitzgerald, D. J., "Ion Thruster Hollow Cathode Studies," in *Supporting Research and Advanced Development,* Space Programs Summary 37, 64, Vol. III. Jet Propulsion Laboratory, Pasadena, Calif., Aug. 31, 1970.

5. King, H. J., and Poeschel, R. L., *Low Specific Impulse Ion Engine,* Final Report, NASA Contract NAS3-11523, Hughes Research Laboratories, Malibu, Calif., Feb. 1970.

6. Rawlin, V. K., and Kerslake, W. R., "Durability of the SERT II Hollow Cathode and Future Applications of Hollow Cathodes," Paper 69-304, Presented at the AIAA 7th Electric Propulsion Conference, Williamsburg, Va., Mar. 1969.

7. Masek, T. D., and Macie, T. W., "Solar Electric Propulsion System Technology," Paper 70-1153, presented at the 8th Electric Propulsion Conference, Stanford, Calif., Aug. 1970.

8. Lidsky, L. M., Rothleder, S. D., Rose, D. J., Yoshikawa, S., Michelson, C., and Mackin, R. J., Jr., "Highly Ionized Hollow Cathode Discharge," *J. Appl. Phys.,* Vol. 33, p. 2490, 1962.

9. Delcroix, J. L., Minoo, H., and Trindade, A. R., "Etablissement D'une Règle Générale Pour Une Décharge D'arc a Cathode Creuse," *J. Phys.,* Vol. 29, p. 605, 1968.

10. Pawlik, E. V., *Performance of a 20-cm Hollow Cathode Ion Thruster,* Technical Memorandum 33-468. Jet Propulsion Laboratory, Pasadena, Calif., Feb. 15, 1971.

11. Pawlik, E. V., and Fitzgerald, D. J., "Cathode and Ion Chamber Investigations on a 20-cm Diameter Hollow Cathode Ion Thruster," Paper 71-158, presented at the AIAA Aerospace Sciences Meeting, New York, Jan. 1971.

12. *Handbuch der Physik,* Vol. 21, Springer-Verlag, Berlin, 1956.

13. Wood, W. P., and Cork, J. M., *Pyrometry,* Second Edition, p. 128. McGraw-Hill Book Co., New York, 1941.

14. Bechtel, R. T., *Discharge Chamber Optimization of the SERT II Thrustor,* NASA TM X-52326, National Aeronautics and Space Administration, Washington, 1967.

15. Levine, J. D., and Gyftopoulos, E. P., "Adsorption Physics of Metals Partially Covered by Metallic Particles. Part III," *Surface Sci.,* Vol. 1, p. 349, 1969.

NASA — JPL — Coml., L.A., Calif.